Effect of Constraining material on the Si-anode nanoparticle in Li-ion Batteries

Project Report submitted to
Indian Institute of Technology, Kharagpur
in partial fulfillment of the requirements for the degree

of

Dual Degree
in Mechanical Engineering - Mechanical Systems Design

by

Ram Hemanth Yeerella
(15ME33028)
&
Boddeda Hemanth Sai Sandeep
(15ME33048)

Under the guidance of

Prof. Jeevanjyoti Chakraborty

DEPARTMENT OF MECHANICAL ENGINEERING
INDIAN INSTITUTE OF TECHNOLOGY KHARAGPUR

CERTIFICATE

This is to certify that the Dissertation Report entitled, "**Effect of Constraining material on the Si-anode nanoparticle in Li-ion batteries**" submitted by "**Mr. Hemanth Sai Sandeep Boddeda**" & "**Mr. Ram Hemanth Yeerella**" to Indian Institute of Technology, Kharagpur, India, is a record of bonafide project work carried out by them under my supervision and guidance and is worthy of consideration for the award of the degree of Bachelor of Technology in Mechanical Engineering of the Institute.

_____

Supervisor

Date:

Declaration

We certify that

a. The work contained in the thesis is original and has been done by us under the guidance of our Supervisor;

b. The work has not been submitted to any other Institute for any degree or diploma;

c. We have followed the guidelines provided by the Institute in preparing the thesis;

d. We have conformed to ethical norms and guidelines while writing the thesis and;

e. Whenever we have used materials (data, models, figures, and text) from other sources, we have given due credit to them by citing them in the text of the thesis, giving their details in the references, and taking permission from the copyright owners of the sources, whenever necessary.

Abstract

A practical scenario of lithium ion diffusion into silicon electrodes is usually associated with traction from surrounding binder material. Using infinitesimal strain theory, a framework to study the mechanical response of a cylindrical silicon anode particle surrounded by an elastic binder in a lithium-ion battery is presented. The electrode is assumed to be under radial traction neglecting any other shear forces at the surface while being axially constrained. It is well known that despite taking measures to prevent fracture of the electrode, the constituent nanoparticles are to fail by buckling. The current framework allows us to investigate this failure using Euler buckling criterion. We incorporate the two-way coupling between stress and Li-ion diffusion in silicon electrode in Fick's law of diffusion. Observations tell us that the stress evolution is dependent on Charging rate, State of charge and the Binder material surrounding electrode. Study facilitate us to find the safe lengths of the electrode to prevent buckling at various states of charge. Results show us that the usage of binder material reinforces electrode thereby facilitates the usage of greater lengths. The model predicts us a minimum state of charge corresponding to the binder elastic modulus before which the buckling never occurs for any length of the electrode. The results can be used to select suitable binder materials which prevent buckling at the onset of charging.

Keywords: Lithium-ion battery, Silicon anode, Two-way coupling, State of Charge, Buckling, Binder

1. Introduction

Modern technological advancements are being constrained by many factors, one of crucial such constraint is the availability of portable large-capacity energy storage devices. Such energy storage devices, for being viable in portable devices, are required to be lightweight, possess a high charge storage capacity and density. Lithium (Li) being the lightest metal leads to a very high energy density of Li-ion batteries making them a suitable choice for portable energy storage devices (Armand and Tarascon 2001; Fletcher 2011; Whittingham 2012). To be used on a large scale and as a replacement of fossil fuels, the lithium-ion batteries are to be used at their highest potential. In lithium-ion batteries, positive electrodes usually metal oxides or phosphates (like $LiCoO_2$, $LiFePO_4$), react with Li via an intercalation mechanism. The strains caused by the insertion of Li atoms into the interstitial sites of eletrode lattice are minimal, and the probable irreversible structural changes are also minimal. In contrast, negative electrode materials such as Si, Sn react with Li via a different mechanism: alloying occurs during lithiation, which involves breaking the bonds between host atoms, causing dramatic structural changes in the process (McDowell et al. 2013). Despite graphite being the most commonly used anode, studies indicate that silicon anode is the most attractive choice owing to its equilibrium phase, $Li_{22}Si_5$ (Gladyeshevskii, Oleksiv, and Kripyakevich 1964). This is superior to graphite as every silicon atom is capable of accommodating 4.4 atoms of Li as opposed to the equilibrium phase of graphite, LiC_6. The equilibrium phase of Si has a higher stoichiometric ratio of Li atoms as the host does not pose any constraint by virtue of its atomic framework, which is modified during the lithiation. It can be noted that graphite electrodes interact with Li via an intercalation mechanism, which explains the lower stoichiometric ratio of Li atoms. The equilibrium phase of lithiated silicon results in high specific capacity of $4200\,\mathrm{mAhg^{-1}}$.

To reach this fully lithiated state, nevertheless, we need to overcome a challenge presented by the massive volumetric change of Si anode accompanying the high intake of charge. The volumetric change at fully lithiated state is greater than 300 % (Beaulieu et al. 2001), and this induces very high stresses, which might lead to mechanical degradation such as fracture or fragmentation of the Si electrode which

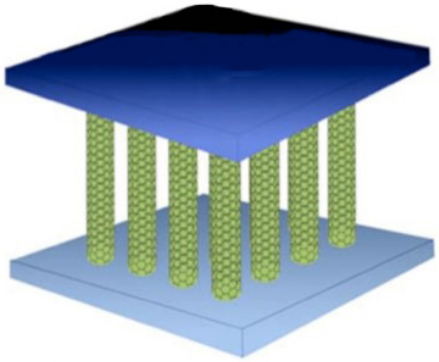

Figure 1.1: A depiction of axially constrained nanowires, ref. Huang et al. 2014

limits the performance of batteries. So it is essential to describe Li-ion diffusion and the diffusion-induced stresses (DIS) adequately. The diffusion process of Li-ions is affected by many factors like concentration gradient, charging rate, stress generated by diffusion of charge and so forth, which is very complex. Each factor affects the diffusion process in a unique way and the charge being diffused into electrode is the cumulative effect of all the factors combined.

Using elastic binders not only helps us put the electrodes in place but also reinforces the electrode. Binders resist the deformation thereby limiting the failure of the electrode. Several works have noted that binder materials need to have high adhesion strength, high stretchability(Chen, Christensen, and Dahn 2003,M. Wu et al. 2013), ductility, electrolyte intake (J. Song et al. 2014), formation of stable SEI layer (Kovalenko et al. 2011,Chong et al. 2011) to offer better cycle life, high coloumbic efficiency and better specific capacity especially for large volume expansion electrode such as Si anodes.

In this work, we try to find out the effect of binder material on the stresses and buckling scenario. We used infinitesimal strain theory, assuming the Li-ion diffusion to be a stress enhanced diffusion considering both concentration gradient as well as hydro-static stress developed in the electrode. We have a two-way coupling between the charge diffusion and the diffusion-induced stresses in Fick's law of diffusion. The electrode is considered to be cylindrical which is concentrically surrounded by elastic binder material that allows charge to diffuse through and is axially constrained that allows no deformation. As the diffusion happens the specific capacity of electrode increases that in turn deforms the electrode and owing to the axial constraint, axial stresses increases leading to a point of failure. The general type of failure for such scenarios is through buckling. Results show us that usage of suitable binder materials prevents the buckling of the electrode also the onset of charging and also aids in the usage of greater lengths.

2. Literature Review

Lithiation of crystalline silicon anodes, or any other negative electrodes, is an example of solid state diffusion involving bulk diffusion as one of the major processes. As substantial volume changes are observed during the lithiation of Si when constrained, they lead to the generation of a higher amount of stresses and can fail. When subjected to repeated cycles of charging/discharging, a silicon anode fails by fracture due to the aforementioned stresses (Kasavajjula, C. Wang, and Appleby 2007; Chan et al. 2011). This kind of failure is prevented by manufacturing nanostructured Si anode particles as the spatial inhomogeneity per se will be lesser in small particles at all charging rates (Park et al. 2009; Chan et al. 2011). Some commonly used nanoparticle geometries are wires, pillars, and tubes. Another way to maintain the capacity and cycle life is to use elastomeric binder materials to hold the particles together (Chen, Christensen, and Dahn 2003; W.-R. Liu et al. 2005)) and the mechanical properties of such binder materials have already been investigated in several works (Chen, Christensen, and Dahn 2003; G. Liu et al. 2008; Chong et al. 2011).

In a battery anode, the nanoparticles are several in number and in addition to the presence of substances like binder, electrolyte and geometrical constraints, they can fail via means other than fracture due to the stress generation. Modeling these modes of failure can aid the battery designers to make better choices in the selection of appropriate materials for the constituents of a battery and certain guidelines regarding the shapes of various components. The investigation of various modes of failure, however, necessitates an understanding of the evolution of stresses inside the anode. Several complicated interactions such as chemical interaction between electrode and electrolyte, spatial constraints to volume changes, chemical interaction of electrode with several other components, varying thermal conditions, irreversible structural and chemical changes are expected to be involved in the generation of stress. However, in simplest of the terms, the practical scenario, in this case, suggests that the time-dependent diffusion that is taking place creates concentration gradients within the solid which correspondingly generates strains.

Prussin (1961) compared stresses caused due to concentration gradients with that of temperature gradients in an otherwise unstressed body and stated that the

corresponding stress is dependent on linear strain coefficient. The stresses arising in an originally unstressed body due to diffusion are termed as diffusion-induced stresses (DIS) or chemical stresses (Prussin 1961; Li 1978). Li (1978) studied the diffusion-induced stresses by proposing and presented their exact solutions for some simple geometries. The foregoing article proves that the chemical stresses always enhance the diffusion, hence the term stress-enhanced diffusion (SED) was coined. Larché and Cahn (1973) derived the coupling of stress and diffusion using thermodynamic considerations wherein the diffusion induce stresses in the body and the stresses affect the diffusion process. Several works subsequently analyzed the evolution of DIS in electrodes of various shapes with either material homogeneity or inhomogeneity while using different formulations of constitutive modeling, along with small deformations, large deformations or plastic deformation analysis (X. Zhang, Shyy, and Sastry 2007; Cheng and Verbrugge 2009; Cheng and Verbrugge 2010; Deshpande, Cheng, and Verbrugge 2010; K. Zhao et al. 2011; Bower, Guduru, and Sethuraman 2011; Y. Song et al. 2012). The chemical potential suggested in the seminal paper by Larché and Cahn (1973) albeit suffers from a limitation as it is only valid for small strains or transformation strains (Cui, Gao, and Qu 2012). It expresses a mathematical expression for chemical flux of an isotropic solute considering the existence of a concentration gradient and stress gradient within a body and defines the appropriate analogous term to the coefficient of thermal expansion.

A linear relation between the strains induced by the diffusion process and the concentration of solute was used to investigate the chemical stresses in a thin plate, within the context of small deformations was investigated by Yang (2005). The formulation used to solve the current problem utilizes the governing equations used in the aforementioned paper in cylindrical polar coordinate geometry to deal with the coupled chemical equilibrium and mechanical equilibrium problem. As we understand that diffusion causes inhomogeneity, we consider a concentration-dependent Young's modulus proposed in (Cui, Gao, and Qu 2012). Cylindrical nanoparticles do not pulverize despite undergoing an increase in diameter and length, unlike other geometries, and can accommodate large strains too (Chan et al. 2011). Therefore, we consider the battery to be made up of several cylindrical nanoparticles.

But this geometry can fail by buckling, another predominant mode of failure, under sufficiently large axial loads while being axially constrained. Such buckling, similar to fracture, may cause capacity deterioration of the anode over several cycles of charging/discharging (Chakraborty et al. 2015). Buckling of an axially constrained nanowire was experimentally observed and for instance, can be seen in Fig. 3 in the work by Chan et al. (2011). Buckling of sufficiently slender cylindrical nanowires was also confirmed by molecular dynamic simulations

discussed in the work by Zang and Y.-P. Zhao (2012b). There are only a few studies addressing the buckling of electrodes arising due to the diffusion-induced stresses. Bhandakkar and Johnson (2012) analyzed the buckling observed in nano-architectured honeycomb structures while Zang and Y.-P. Zhao (2012a) studied the self-buckling induced by surface stresses in hollow nanospheres and nanotubes. A thorough investigation of buckling of axially constrained cylindrical nanoparticles with traction-free surfaces was carried out by (Chakraborty et al. 2015) wherein they considered a two-way coupling between stress and diffusion along with plastic deformations. They were able to predict a critical length beyond which buckling do not occur for a given radius of the specimen. Another recent contribution to the buckling problem was made by (K. Zhang et al. 2017) where they carried out large deformation analysis and compared those results with the results obtained using linear theory, and proposed an estimate for the validity of linear theory to estimate the critical length for buckling.

The binder, which occupies as much as 50% of the battery weight (Singh and Bhandakkar 2017), when used along with nanoparticles can be the major constituent that restricts the radial growth of the nanoparticles during diffusion. There are few works where either the effects of binder on the evolution of stress was investigated or the binder and anode particles are treated as a composite to observe the stress profiles in both of them. W. Wu et al. (2014) developed a microstructural resolved model of Li-ion battery cell with graphite as anode, incorporating the species transport, battery kinetics, covered by a perfectly conductive binder to study the stress distribution in binder and active particles. Higa and Srinivasan (2015) presented a finite-deformation model to observe the mechanical interactions between an amorphous anodic silicon particle undergoing lithium insertion and attached binder material. They used an axisymmetric model and explored the influence of active material size and binder stiffness on von Mises stress. Takahashi et al. (2016) showed that the stresses generated in a graphite anode when used in conjunction with PVDF binder are small enough to prevent cracks. Their model assumed a spherical anode and binder composite with the particle radius and binder remaining constant during the lithiation and delithiation, which was facilitated by the fact that graphite suffers small deformations. The above two models assumed elastic behavior of binder while a viscoelastic binder behavior was considered in the works by Santimetaneedol et al. (2016) and Singh and Bhandakkar (2017). These articles investigated the stresses in binders that can exhibit either viscoelastic behavior or elastic-viscoplastic behavior and its effect on electrode which is undergoing lithiation/delithiation. However, to the best knowledge of the current authors' a formal study on the influence of binder on the buckling of electrode nanoparticles is yet to be undertaken.

3. Mathematical Model

In this report, we consider a pristine silicon nanoparticle embedded in a binder matrix. A characteristic of Si anodes undergoing lithiation is that electrochemically-driven solid-state amorphization occurs within the initial cycles of charging i.e., a transformation from crystalline to disordered phases takes place (Limthongkul et al. 2003). Therefore, a amorhpus silicon nanoparticle is considered, and this enables us to treat it is an istropic solid. We consider a cylindrical nanoparticle and this geometry has been observed to withstand pulverization. An interesting result to mention is that the stresses in the binder remain unaffected irrespective of the material behavior of the electrode i.e, elastic, elastic-perfectly plastic (Singh and Bhandakkar 2017). Therefore, we treat the nanowire as a homogeneous elastic solid. This nanoparticle is assumed to be embedded inside a binder matrix which is capable of offering radial traction. The shear tractions at the surface are neglected. We do not extend our investigation to the stresses generated in the binder. In the current model, the effect of the surrounding binder matrix is acting as a radial constraint by offering a resistance proportional to the non-dimensional radial deformation of the nanowire while considering the diffusion process. The whole study is based on the infinitesimal strain assumption used in the theory of linear elasticity. We would like to note here that despite silicon undergoing large deformations, small elastic strains takes place as plastic deformation accommodates for the large volume changes (Chakraborty et al. 2015). Therefore, our current modeling of the mechanical response of the nanoparticle while undergoing diffusion is based on the analogy of the current problem with linear thermoelasticity. As the contribution from axial diffusion for buckling is found to be negligible even for small slenderness ratio(K. Zhang et al. 2017), the nanoparticle is only subjected to radial diffusion and the end effects are neglected, ref Fig. 3.1 (Hao et al. 2012). The entire diffusion process is taken to be axisymmetric. We ignore the chemical interactions between electrolyte and electrode. We would like to state that binder is completely permeable to lithium and no chemical interaction is considered between the lithium and binder. An additional assumption is that radial variations are greater than those in the axial direction. The model incorporates the two-way coupling of stress and diffusion, i.e., both diffusion-induced stress (DIS) and

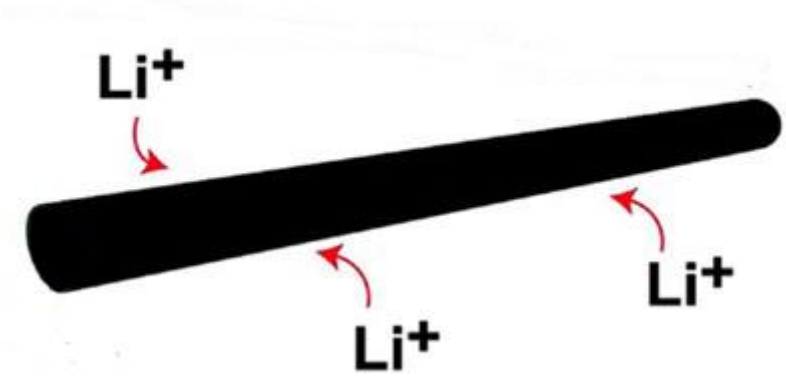

Figure 3.1: A depiction of lithiation

stress-enhanced diffusion (SED) are included. Fick's law of diffusion are used for modeling the mass transport process with a modified chemical potential. To carry out the buckling analysis, the cylinder is treated as a beam with hinged ends and Euler buckling criterion is used. The binder is assumed to offer a uniform transverse resistive force that is proportional to the Therefore, we would like to consider the buckling of cylindrical nanoparticles embedded in binder matrix using linear theory of elasticity and Euler buckling criterion. The beam column experiences a uniform transverse resistive force offered by the binder that is proportional to the transverse deflection of the beam.

3.1 Diffusion

Let $c(r,t)$ represent the concentration field of a charging (or discharging) electrode as a function of radial position r, at any instant t, where $t = 0$ is set at the inception of charging (or discharging). If J is the flux, then following Fick's second law of Diffusion, we write

$$\frac{\partial c}{\partial t} = -\frac{1}{r}\frac{\partial (rJ)}{\partial r} \tag{3.1}$$

From the thermodynamic considerations, the flux of Li, J can be related to chemical potential, μ as follows,

$$J = -Mc\nabla\mu \tag{3.2}$$

where M is the mobility of solute atoms, and ∇ is the gradient operator in cylindrical polar coordinates. Upon assuming that the solute (Li) concentration is not high, we can use the chemical potential proposed by Li 1978 pertaining to the

chemical potential for dilute solutions.

$$\mu = \mu_0 + R_g T \ln(c) - \Omega \sigma_{hyd} \tag{3.3}$$

where μ_0 is a constant, R_g is the universal gas constant, T is the absolute temperature, Ω is the partial molar volume of solute, and σ_{hyd} is the hydrostatic state of stress, and is the mean of the principal stresses represented by σ_{rr}, $\sigma_{\theta\theta}$, σ_{zz}. Substituting these equations (3.2) and (3.3) in (3.1), we obtain the following equation

$$\frac{\partial c}{\partial t} - \frac{1}{r}\frac{\partial}{\partial r}\left\{ r\left(D_0 \frac{\partial c}{\partial r} - M\Omega \frac{\partial \sigma_{hyd}}{\partial r} \right) \right\} = 0 \tag{3.4}$$

Here, D_0 is the diffusivity of silicon and is related to the mobility of the solute atoms by the following relation, $D_0 = MR_gT$. As the nanoparticle did not contain any lithium initially, we have

$$c(r, 0) = 0 \tag{3.5}$$

Axisymmetric radial diffusion implies

$$J(0, t) = 0 \tag{3.6}$$

Upon considering a self-limiting lithiation, we obtain the boundary condition indicating the flux at periphery as (Cui, Gao, and Qu 2012)

$$J|_{r=R_0} = J_0(1 - \tilde{c}|_{\tilde{r}=1}) \tag{3.7}$$

where J_0 corresponds to the charging rate and $\tilde{c}$ is the non-dimensional concentration of lithium.

3.2 Mechanical Equilibrium

We use the same constitutive equations coupling concentration and deformation associated transformation strains, proposed by X. Zhang, Shyy, and Sastry 2007.

$$\begin{cases} \epsilon_{rr} = & \frac{1}{E}[\sigma_{rr} - \nu\,(\sigma_{\theta\theta} + \sigma_{zz})] + \frac{1}{3}\Omega c(r,t) \\ \epsilon_{\theta\theta} = & \frac{1}{E}[\sigma_{\theta\theta} - \nu\,(\sigma_{rr} + \sigma_{zz})] + \frac{1}{3}\Omega c(r,t) \\ \epsilon_{zz} = & \frac{1}{E}[\sigma_{zz} - \nu\,(\sigma_{\theta\theta} + \sigma_{rr})] + \frac{1}{3}\Omega c(r,t) \end{cases} \tag{3.8}$$

where ϵ_{rr}, $\epsilon_{\theta\theta}$, and ϵ_{zz} are the principal strain components, and σ_{rr}, $\sigma_{\theta\theta}$, and σ_{zz} are principal stress components along the radial, hoop, and axial directions, respectively. The Young's modulus, denoted by E, is concentration dependent. We use the same relation for Young's modulus given by Cui, Gao, and Qu (2012)

$$E = E_0(1 + \eta_E \chi_{\max} \tilde{c}) \tag{3.9}$$

In cylindrical polar coordinate system, the strain components are related to the displacement vector $\mathbf{u} \equiv [u, v, w]^{\mathrm{T}}$ as

$$\epsilon_{rr} = \frac{\partial u}{\partial r}, \qquad \epsilon_{\theta\theta} = \frac{u}{r}, \qquad \epsilon_{zz} = \frac{\partial w}{\partial z} \tag{3.10}$$

We consider a long cylinder resulting in the plane strain assumption(Deshpande, Cheng, and Verbrugge 2010).

$$\epsilon_{zz} = 0 \tag{3.11}$$

Assuming axisymmetry of the diffusion process and subsequent growth of the cylinder, we can write the following mechanical equilibrium equation.

$$\frac{\partial \sigma_{rr}}{\partial r} + \frac{\sigma_{rr} - \sigma_{\theta\theta}}{r} = 0 \tag{3.12}$$

We would like to note here that axisymmetry implies lack of shear strains and similarly corresponding shear stresses. The radial displacement along the axis of the cylinder is zero throughout the diffusion process, and is a result of the axisymmetry. We approximate that the binder offers a resisting pressure that is linearly proportional to the non-dimensional radial displacement, $\tilde{u}$ at periphery. As a result, we obtain the following boundary conditions pertaining the governing PDE of mechanical equilibrium.

$$u|_{r=0} = 0, \qquad \sigma_{rr}|_{r=R_0} = E_b \tilde{u}|_{\tilde{r}=1} \tag{3.13}$$

Here, E_b is the binder Young's modulus and $\tilde{u}$ is the non-dimensional radial displacement.

3.3 Non-dimensionalization

We use the following non-dimensionalization scheme.

$$\begin{aligned} &\tilde{r} = \frac{r}{R_0}; \qquad \tilde{t} = \frac{t}{R_0^2/D_0}; \qquad \tilde{u} = \frac{u}{R_0}; \qquad \tilde{w} = \frac{w}{L_0}; \\ &\tilde{c} = \frac{c}{c_{\mathrm{ref}}}; \qquad \tilde{\sigma}_{rr,\theta\theta,zz,hyd} = \frac{\sigma_{rr,\theta\theta,zz,hyd}}{\Omega E_0 c_{\mathrm{ref}}}; \qquad \tilde{J} = -\frac{\partial \tilde{c}}{\partial \tilde{r}} + \frac{\Omega^2 E_0 c_{\mathrm{ref}}}{R_g T} \tilde{c} \frac{\partial \tilde{\sigma}_{hyd}}{\partial \tilde{r}} \end{aligned} \tag{3.14}$$

Upon non-dimensionalizing (3.1), (3.12) ,and their corresponding initial and boundary conditions, we obtain

$$\frac{\partial \tilde{c}}{\partial \tilde{t}} = -\frac{1}{\tilde{r}} \frac{\partial (\tilde{r} \tilde{J})}{\partial \tilde{r}} \tag{3.15}$$

$$\tilde{J} = \frac{J_0}{D_0 c_{\text{ref}}/R_0}(1-\tilde{c}); \qquad \tilde{J}(0,\tilde{t}) = 0; \qquad \tilde{c}(\tilde{r},0) = 0 \tag{3.16}$$

$$\frac{\partial \tilde{\sigma}_{rr}}{\partial \tilde{r}} + \frac{\tilde{\sigma}_{rr} - \tilde{\sigma}_{\theta\theta}}{\tilde{r}} = 0 \tag{3.17}$$

$$\tilde{u}\big|_{\tilde{r}=0} = 0; \qquad \tilde{\sigma}_{rr}\big|_{\tilde{r}=1} = \frac{E_b}{\Omega E_0 c_{\text{ref}}}\tilde{u}\big|_{\tilde{r}=1} \tag{3.18}$$

We would like to note here that non-dimensional charging rate is denoted by ξ. Hence, the non-dimensional boundary condition at the periphery corresponding to diffusion equation reads as

$$\tilde{J}|_{\tilde{r}=1} = \xi(1-\tilde{c})|_{\tilde{r}=1}; \qquad \xi = \frac{J_0}{D_0 c_{\text{ref}}/R_0} \tag{3.19}$$

3.4 Buckling

As the nanoparticle is axially constrained; along with the increasing stresses during lithiation, there is a possibility of buckling for some length. We treat this problem by approximating the situation to a beam column with pinned-pinned ends. The beam column experiences a uniform transverse resistive force offered by the binder that is proportional to the transverse deflection of the beam, denoted by y. The corresponding equation related to the bending can be written as follows

$$EI\frac{\mathrm{d}^4 y}{\mathrm{d}z^4} + p\frac{\mathrm{d}^2 y}{\mathrm{d}z^2} = -2E_b y \tag{3.20}$$

where EI is the flexural rigidity of the cylinder and p is the resultant axial force obtained by integrating axial stress over the circular cross-sectional area. Solving the above equation (3.20), we obtain the following solution

$$\frac{pL_0^2}{EI} = n^2\pi^2 + \frac{2E_b L_0^4}{n^2\pi^2 EI} \tag{3.21}$$

We have

$$\begin{aligned} p &= \Omega E_0 c_{\text{ref}} R_0^2\ \tilde{p}; \qquad \tilde{p} = \int_0^1 \tilde{\sigma}_{zz} 2\pi\tilde{r}\,\mathrm{d}\tilde{r}; \\ EI &= 4R_0^4 E_0 \widetilde{EI}; \qquad \widetilde{EI} = \frac{\pi}{8}\int_0^1 \tilde{r}^3\left(1+\eta_E\chi_{\max}\tilde{c}(\tilde{r},\tilde{t}\right)\mathrm{d}\tilde{r} \end{aligned} \tag{3.22}$$

Its corresponding non-dimensional form is given by

$$\tilde{p} = \frac{4n^2\pi^2}{\Omega c_{\text{ref}}\lambda^2}\widetilde{EI} + \frac{2E_b\lambda^2}{\Omega E_0 c_{\text{ref}} n^2\pi^2} \tag{3.23}$$

Table 3.1: Values of material properties and operating parameters

Parameter	Symbol	Value
Radius of the nanoparticle	R_0	$200\,\mathrm{nm}$
Temperature	T	$300\,\mathrm{K}$
Universal gas constant	R_g	$8.314\,\mathrm{J\,K^{-1}\,mol^{-1}}$
Diffusivity of Si	D_0	$1 \times 10^{-16}\,\mathrm{m^2\,s^{-1}}$[a]
Maximum stoichiometric Li concentration	c_{ref}	$53.398\,\mathrm{molecule/nm^{-3}}$ [b]
Modulus of elasticity of pure Si	E_0	$90.13\,\mathrm{GPa}$[c]
Partial molar volume of solute	Ω	$0.014\,\mathrm{nm^3\,molecule^{-1}}$ [b]
Rate of change of modulus of elasticity with concentration	η_E	-0.1464 [d]
Maximum concentration of Li in Si	$\chi_{\max}$	4.4 [e]
Poisson's ratio	ν	0.28 [d]

Here, n indicates the buckling mode, λ indicates the slenderness ratio, which is defined as the ratio of length to radius i.e., $\lambda = \dfrac{L_0}{R_0}$. Since the axial stress generated are continuous with time and from the equation we understand that for higher modes of buckling critical electrode length turns out to be higher, so we study only first order buckling as it is the most conservative estimate.

[a] Ding et al. 2009
[b] Boukamp, Lesh, and Huggins 1981
[c] Rhodes et al. 2010
[d] Cui, Gao, and Qu 2012
[e] Chakraborty et al. 2015

4. Results

We used COMSOL Multiphysics finite element package to numerically solve the coupled non-linear partial differential equations given by (3.15) and (3.17). The simulation was run with a stop condition that stops when the specific capacity reaches $3900\,\mathrm{mAhg}^{-1}$. This stop condition was set to eliminate erroneous results (discontinuities, steep curves) indicating higher non-dimensional concentrations ($\tilde{c} > 1$), which is caused by the lack of convergence in the solver. Upon obtaining the concentration and deformation fields, we solved the biquadratic equation in λ obtained from (3.23) only considering the first buckling mode. State of Charge denoted by SOC is used to represent the results and it is computed as $SOC = 4200 \int_0^1 \tilde{c}\; 2\pi\tilde{r}\,\mathrm{d}\tilde{r}$.

Figure 4.1 depict the variation of radial, hoop and axial stress with radial coordinates under different conditions at 50% SOC.

Figures 4.1a and 4.1b corresponds to plots of radial stresses, it is highly tensile during centre of the electrode and slowly relaxes. If there is no binder surrounding the electrode, radial stress relaxes to zero at the periphery where as when the electrode is surrounded by a binder material of some specific elastic modulus radial stress becomes compressive near to periphery and its value is proportional to the elastic modulus of the binder. This is in accordance with the pressure boundary condition at periphery. Figures show variation with different charging rates and we observe that the magnitude of radial stress is increasing with increase in charging rate for both with and without binder.

Figures 4.1c and 4.1d corresponds to plots of hoop stresses, for both with and without binder material they change from tensile at the centre relaxes as we move along the radius and nearing periphery becomes compressive. If we rearrange the equilibrium condition we can write hoop stress as sum of radial stress and its spatial gradient multiplied with distance from centre. As we move along radius the tensile radial stresses becomes less tensile while its spatial gradient is negative thus making the plot of hoop stress vs radius change its nature from tensile to compressive.In the absence of binder material, the variation with charging rates for both radial and hoop stresses is similar, the curves are scaled for different charging rates and as the charging rate increases they are scaled with higher values. The change of

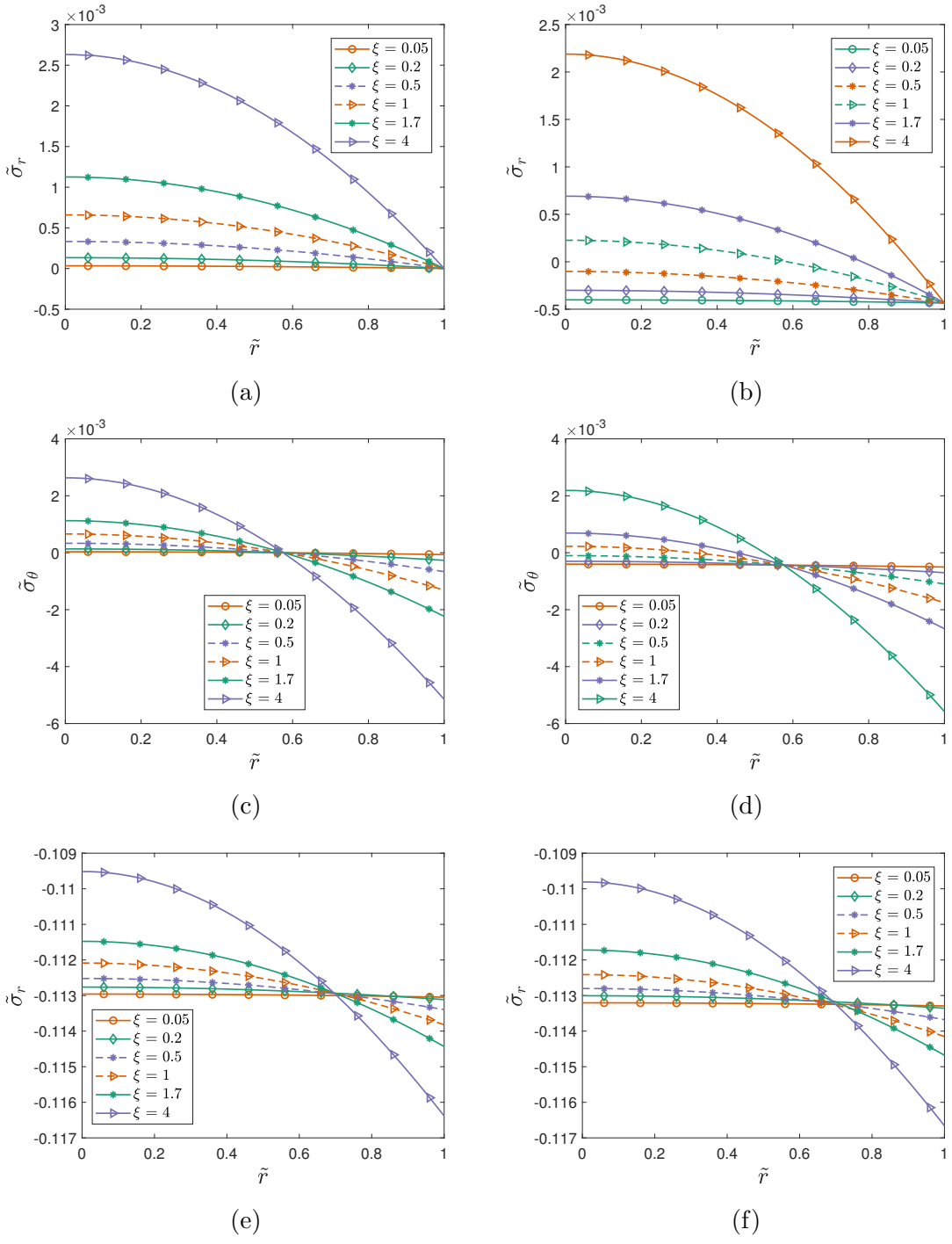

Figure 4.1: Influence of charging rate on stresses considering the absence of binder and presence of a binder. The plots on the left are for $E_b = 0\,\text{MPa}$ while the plots on right depict the case with $E_b = 184\,\text{MPa}$ both at 50% state of charge

hoop stress from tensile to compressive occurs near the midpoint. On speculation, if electrode without binder is considered as the reference case, we can say that the radial stresses and hoop stresses (vs) radius plots for various charging rates as a whole seem like shifting downwards (decrease in value along y-axis) when a binder material is present. The amount of shift is proportional to the strength of binder. Figures 4.1e and 4.1f shows plots of axial stresses, here we find no significant difference for an electrode with and without binder material. At lower charging rates the axial stresses are nearly uniform with radius and as we increase charging rate it becomes more compressive near the periphery than compared to the centre, but this change is so small to be considered(less than 8 %). So, we can say axial stresses does not vary much with charging rates and strength of binder material.

The radial and hoop stresses curves with time initially increase to a higher magnitude and then slowly relaxes and decrease to a some constant asymptotic value, whereas the axial force always increase with time and finally attains an asymptotic value slightly lower than the maximum value. It compressive nature is due to the boundary condition which does not allow for any deformation along the axial direction.

Figure 4.2 shows the variation of stresses with time with and without a binder at different radial values for a charging rate 1. The radial stresses as said earlier first reaches a peak value and then relaxes, the time that takes to attain a peak depends on the charging rate and the asymptotic value depends on the binder elastic strength. If there is no binder present then the tensile radial stress relaxes to zero but if a binder material is present the stresses slowly becomes compressive and their magnitude is proportional to the elastic modulus of the binder. From the speculations of Figure 4.1, we know that the radial stress as we move from centre to periphery relaxes from tensile to zero or slightly compressive depending on the binder's elastic modulus. So the peaks in stress vs time plots, we have higher peak magnitude for lower radial points but as the time increases and SOC of electrode increase all the radial points have nearly the same stress value.
Hoop stress also have a similar trend to that of radial stress, from figure 4.1 we see that hoop stress as we go from centre to periphery becomes tensile to compressive so the hoop stress vs time plots have different curves for radial points near centre and near periphery. Points near to centre are similar as of radial stresses but the points near periphery first attains a peak compressive value and then relaxes to a lesser compressive value and at a later time. In a broad view, there isn't much difference in the axial stresses with radial points as well as with binder elastic modulus which is a similar speculation form that of figure 4.1. Only upon a close inspection we observe that at higher state of charge axial stress for electrode with binder are slightly higher than that of the electrode without any binder material surrounding it.

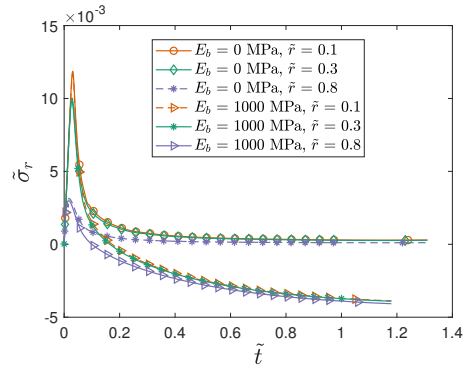

(a)

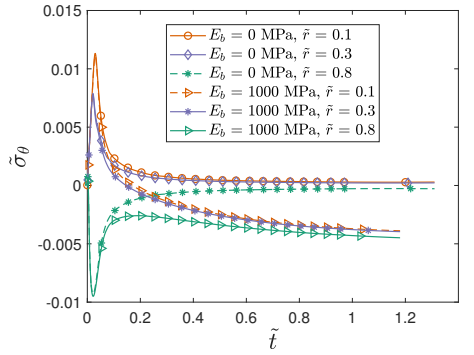

(b)

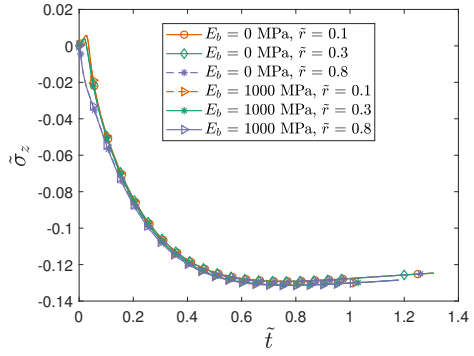

(c)

Figure 4.2: Variation of stresses with time, $\xi = 1$

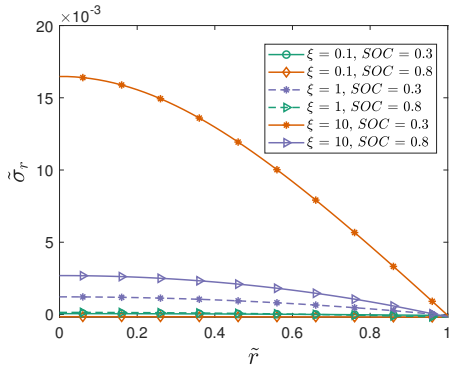

(a)

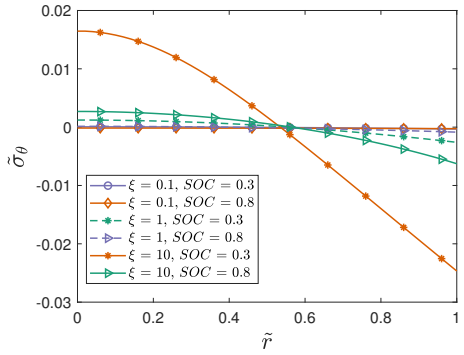

(b)

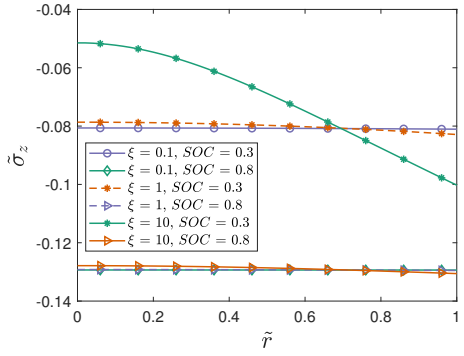

(c)

Figure 4.3: Variation of stresses with radius, $E_b = 50\,\mathrm{MPa}$

The relaxation of stresses with time can be reasoned with the increase in the charge inside the electrode decreases the charge gradient inside electrode and the radial and hoop stresses that are majorly affected by charge diffusion decreases. Where as the axial stresses goes on increasing as the amount of charge increases and owing to constraint on its axial growth which allows no deformation.

Figure 4.3 represent the development of stresses in an electrode surrounded by a binder of Young's modulus equal to 50 MPa with radius and time respectively. The plots which show the variation with radius are drawn for different charging rates at two different instants where the state of charge in the electrode reaches 30% and 80% respectively. Figure 4.3a shows that the radial stress at the periphery is same for a given state of charge irrespective of the charging rate, which is in accordance with the uniform, time-varying pressure boundary condition at the periphery. At very low charging rate ($\xi = 0.1$), we observe that the radial stresses become entirely compressive beyond a state of charge. The magnitude of these compressive radial stresses is dependent on the binder modulus. If we observe figures 4.1a and 4.1b, we can see that the presence of binder cause the radial stresses to become compressive at least for some region closer to the periphery. From figure 4.1a, we observe that for a given state of charge, as the charging rate increases the radial stress increases. This phenomenon when compared with figure 4.1b, it is clear that such diffusion-induced tensile radial stresses will resist the compressive pressure exerted by the binder leading to a net tensile nature of the radial stress in the inner shells. However, for lower charging rates and for sufficiently high state of charge, owing to the low diffusion-induced stresses and higher compressive pressure of the binder, we observe compressive radial stresses throughout the cross-section. The magnitude of this compressive stress increases from the center to the periphery, owing to the fact that the binder exerts its pressure at the periphery. Figure 4.3b shows that the cylindrical shells closer to the center experience tensile hoop stress while the outer shells experience compressive hoop stress. The radial coordinates at which such transition from tensile to compressive nature occur does not have a fixed trend. If we consider the plots corresponding to the non-dimensional charging rates 1 and 10, we observe that at lower state of charge, larger region experiences tensile hoop stress for lower charging rates while at higher state of charge, higher charging rate results in larger region experiencing the tensile hoop stress. It is also noted that for low charging rate viz., $\xi = 0.1$, at a high state of charge such as 0.8, we have a uniform compressive stress. Figure 4.3c clearly indicates that axial stresses at higher state of charge are highly compressive irrespective of the charging rate. We observe that at both times, greater compressive stresses are observed closer to the periphery for any charging rate.

From figure 4.4, we observe a general property that the maximum length to

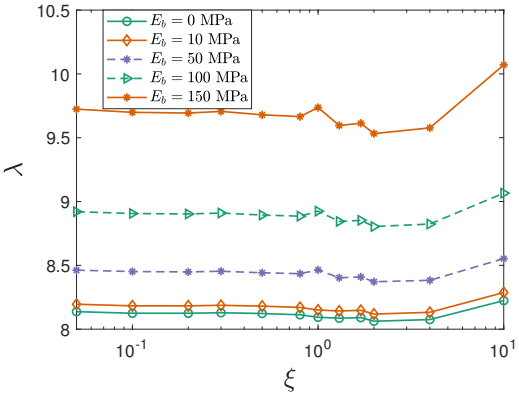

(a) State of Charge - 15%

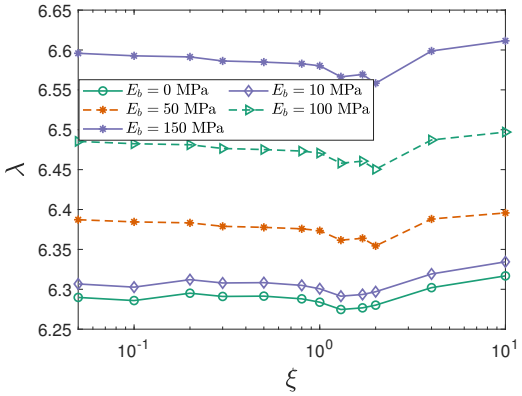

(b) State of Charge - 25%

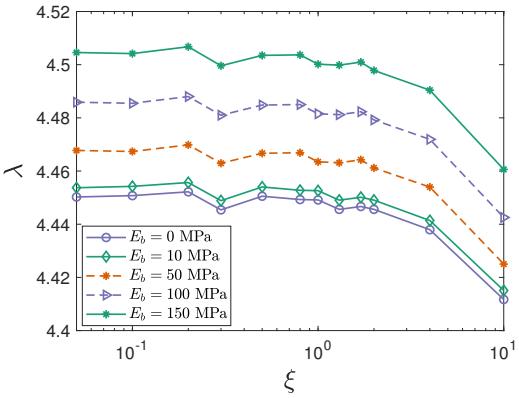

(c) State of Charge - 50%

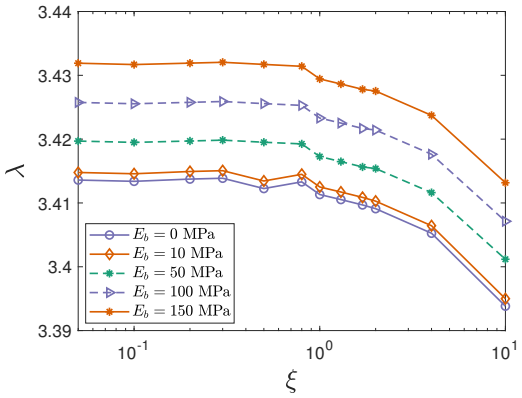

(d) State of Charge - 85%

Figure 4.4: Variation of maximum slenderness ratio to avoid buckling with charging rate for binders with different elastic modulus and state of charge

radius ratio (slenderness ratio) of an electrode that can be used before it buckles at any specific SOC increases with increase in the binder elastic modulus. Similarly the max length of the electrode that can withstand the Li-ion diffusion without buckling decreases with an increase in the capacity of the electrode. The latter property can be attributed to the fact that as the State of Charge increases the stresses generated in electrodes increase thereby to withstand a higher buckling load length of the electrode is to be decreased. The above phenomenon can be realized as the increase in binder elastic modulus helps electrode (acting as a shield and preventing failures) withstand the buckling load for higher lengths. Upon close inspection, we observe that the slenderness ratio vs charging rate curves has different nature for higher and lower capacities. The buckling lengths do not differ much with charging rate up to ξ=1, but at lower capacities (less than 50% SOC), length increases with charging rate whereas at higher capacities (greater than 50% SOC) the length decreases with an increase of charging rate. Conjecture is that when an electrode is at lower capacity and with higher charging rate the charge gradient in the electrode is less thus stress is a bit lower thereby allowing for greater lengths than that at the lower charging rates.

From figure 4.5a, we can clearly observe that the specimen surrounded by a binder with $E_b = 1000\,\mathrm{MPa}$, does not buckle for any length if the desired SOC is 15% or 25%, which implies that the length can be arbitrarily increased in an unbounded manner for any given finite radius. Upon observing the figures 4.4(c) and 4.4(d), we find that the difference between the maximum and minimum of slenderness ratio values seen for the highest and least binder modulus respectively decreases with an increase in the required SOC. As with higher lithium concentration inside the electrode, the concentration-dependent strain induced stresses attain significant values causing buckling to occur at lower slenderness ratio than the scenario where binder strength is the single major factor in deciding the length for the onset of buckling. Therefore, we observe this lower slenderness ratio spread with an increase in SOC.

From our first observation that at any given capacity the slenderness ratio for buckling increases with an increase in binder elastic modulus, we slowly attain a point where the electrode does not buckle for any length (slenderness ratio tends to infinity) at some higher elastic modulus binder. In the same way, there exists a minimum value of SOC for an electrode to buckle which is surrounded by binder material with a specific elastic modulus. This minimum SOC can be seen in Figure4.5a, we observe that as the magnitude of binder's elastic modulus increases, the minimum SOC required for the buckling to happen increases. Thus we can get for a higher elastic modulus binder (say greater than 2 GPa) the electrode will never buckle for any charge capacity. Subsequently, from Figure 4.5b we can see the critical slenderness ratio value at the tipping condition from the non-

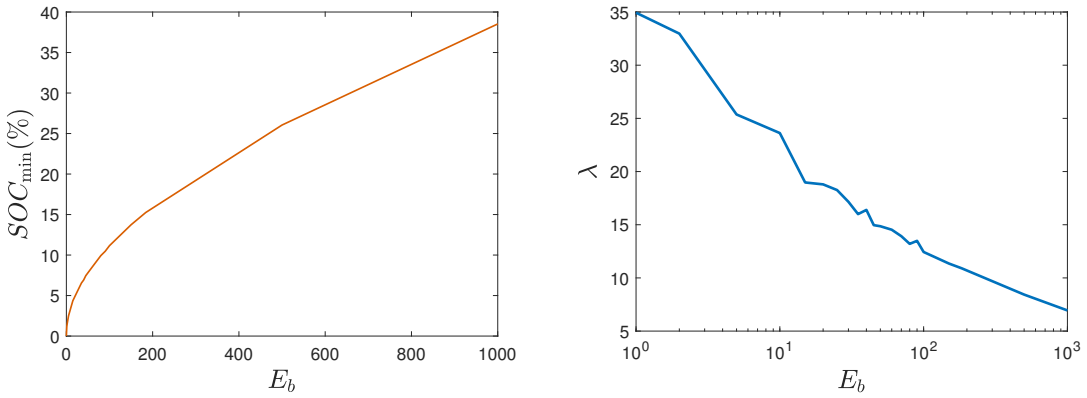

(a) (b)

Figure 4.5: Variation of Maximum critical slenderness ratio and the corresponding SOC with binder's Young's modulus. Both figures correspond to non-dimensional charging rate = 1

buckling regime to buckling regime (corresponding with SOC). This critical value of lambda (slenderness ratio) at the tipping point decreases with the increase in binder modulus as the corresponding SOC required for buckling is higher.

Figure 4.6 depicts the variation of buckling time with charging rate for a fixed length to radius ratio of the undeformed specimen and it reiterates the fact that lower slenderness ratio is required to prevent premature buckling, i.e. buckling at a low state of charge. There are slight variations in the SOC at which buckling occurs for a given From the figure; it is clear that the state of charge along with the governs the buckling length and charging rate has little to no influence over it. However, to attain a given state of charge, the time required would depend on the charging rate. So, charging rate decides the time at which the onset of buckling occurs, and the accumulated Li atoms inside the nanoparticle decide the buckling length.

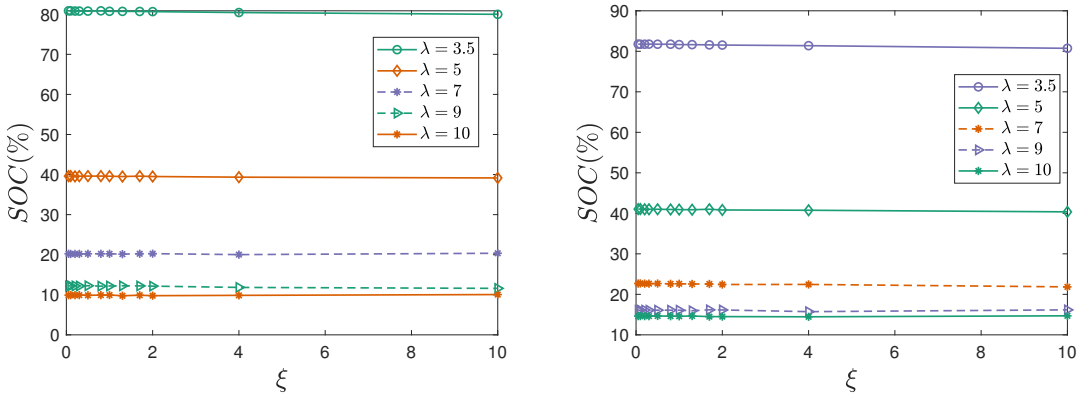

(a) Without any binder material (b) Binder of elastic modulus 150 MPa

Figure 4.6: Variation of state of charge at buckling with charging rates for various slenderness ratios

Conclusions & Future Scope

We have analytically investigated the influence of binder on the critical length required for buckling of cylindrical nanoparticles. The nanoparticle is modeled as a elastic solid. It is assumed homogeneous, isotropic solid undergoing axisymmetric, infinitesimal deformation during the bulk diffusion process. The binder is completely permeable to Li-ion and a self-limiting lithiation mechanism takes place at the surface of the nanoparticle. The binder is assumed to offer radial traction at the electrode surface and a resistive pressure to the transverse deflections. From the results we clearly observe that the usage of binder helps us exploit high charge capacity of the Li-ion batteries by reducing the risk of failures. From the observations of radial stress plots we understand that the usage of binder materials reduce the high tensile stresses generated. We can use greater electrode length (an increase of more than 10% if the buckling occurs at 50% specific capacity) while safeguarding against buckling even at higher capacities as well as prevent any possibilities of failure by buckling at the onset of charging.

The work can be extend further by considering shear traction along with radial traction. Diffusion of Li-ions in all directions i.e., axial diffusion along with radial diffusion can be incorporated in charge diffusion thereby making a complete study of 3-D model. Incorporating large deformation analysis in the place of infinitesimal strain theory. We can also try extending the study by prying into plastic regime.

Bibliography

Armand, M and JM Tarascon (2001). "Issues and challenges facing rechargeable batteries". In: *Nature* 414, pp. 359–367.

Beaulieu, LY, KW Eberman, RL Turner, LJ Krause, and JR Dahn (2001). "Colossal reversible volume changes in lithium alloys". In: *Electrochemical and Solid-State Letters* 4.9, A137–A140.

Bhandakkar, Tanmay K and Harley T Johnson (2012). "Diffusion induced stresses in buckling battery electrodes". In: *Journal of the Mechanics and Physics of Solids* 60.6, pp. 1103–1121.

Boukamp, BA, GC Lesh, and RA Huggins (1981). "All-solid lithium electrodes with mixed-conductor matrix". In: *Journal of the Electrochemical Society* 128.4, pp. 725–729.

Bower, Allan F, Pradeep R Guduru, and Vijay A Sethuraman (2011). "A finite strain model of stress, diffusion, plastic flow, and electrochemical reactions in a lithium-ion half-cell". In: *Journal of the Mechanics and Physics of Solids* 59.4, pp. 804–828.

Chakraborty, Jeevanjyoti, Colin P Please, Alain Goriely, and S Jonathan Chapman (2015). "Combining mechanical and chemical effects in the deformation and failure of a cylindrical electrode particle in a Li-ion battery". In: *International Journal of Solids and Structures* 54, pp. 66–81.

Chan, Candace K, Hailin Peng, Gao Liu, Kevin McIlwrath, Xiao Feng Zhang, Robert A Huggins, and Yi Cui (2011). "High-performance lithium battery anodes using silicon nanowires". In: *Materials for Sustainable Energy: A Collection of Peer-Reviewed Research and Review Articles from Nature Publishing Group*. World Scientific, pp. 187–191.

Chen, Zonghai, L Christensen, and JR Dahn (2003). "Large-volume-change electrodes for Li-ion batteries of amorphous alloy particles held by elastomeric tethers". In: *Electrochemistry communications* 5.11, pp. 919–923.

Cheng, Yang-Tse and Mark W Verbrugge (2009). "Evolution of stress within a spherical insertion electrode particle under potentiostatic and galvanostatic operation". In: *Journal of Power Sources* 190.2, pp. 453–460.

Cheng, Yang-Tse and Mark W Verbrugge (2010). "Diffusion-induced stress, interfacial charge transfer, and criteria for avoiding crack initiation of electrode particles". In: *Journal of the Electrochemical Society* 157.4, A508–A516.

Chong, Jin, Shidi Xun, Honghe Zheng, Xiangyun Song, Gao Liu, Paul Ridgway, Ji Qiang Wang, and Vincent S Battaglia (2011). "A comparative study of polyacrylic acid and poly (vinylidene difluoride) binders for spherical natural graphite/LiFePO4 electrodes and cells". In: *Journal of power sources* 196.18, pp. 7707–7714.

Cui, Zhiwei, Feng Gao, and Jianmin Qu (2012). "A finite deformation stress-dependent chemical potential and its applications to lithium ion batteries". In: *Journal of the Mechanics and Physics of Solids* 60.7, pp. 1280–1295.

Deshpande, Rutooj, Yang-Tse Cheng, and Mark W Verbrugge (2010). "Modeling diffusion-induced stress in nanowire electrode structures". In: *Journal of Power Sources* 195.15, pp. 5081–5088.

Ding, N, J Xu, YX Yao, Gerhard Wegner, X Fang, CH Chen, and Ingo Lieberwirth (2009). "Determination of the diffusion coefficient of lithium ions in nano-Si". In: *Solid State Ionics* 180.2-3, pp. 222–225.

Fletcher, Seth (2011). *Bottled lightning: superbatteries, electric cars, and the new lithium economy*. Hill and Wang.

Gladyeshevskii, EI, GI Oleksiv, and PI Kripyakevich (1964). "New examples of structural type $Li_{22}Pb_5$". In: *Soviet Physics Crystallography, USSR* 9.3, p. 269.

Hao, Feng, Pei Dong, Jing Zhang, Yongchang Zhang, Phillip E Loya, Robert H Hauge, Jianbao Li, Jun Lou, and Hong Lin (2012). "High electrocatalytic activity of vertically aligned single-walled carbon nanotubes towards sulfide redox shuttles". In: *Scientific reports* 2, p. 368.

Higa, Kenneth and Venkat Srinivasan (2015). "Stress and strain in silicon electrode models". In: *Journal of The Electrochemical Society* 162.6, A1111–A1122.

Huang, Lei, Qiulong Wei, Ruimin Sun, and Liqiang Mai (2014). "Nanowire Electrodes for Advanced Lithium Batteries". In: *Frontiers in Energy Research* 2, p. 43. ISSN: 2296-598X. DOI: 10.3389/fenrg.2014.00043. URL: https://www.frontiersin.org/article/10.3389/fenrg.2014.00043.

Kasavajjula, Uday, Chunsheng Wang, and A John Appleby (2007). "Nano-and bulk-silicon-based insertion anodes for lithium-ion secondary cells". In: *Journal of Power Sources* 163.2, pp. 1003–1039.

Kovalenko, Igor, Bogdan Zdyrko, Alexandre Magasinski, Benjamin Hertzberg, Zoran Milicev, Ruslan Burtovyy, Igor Luzinov, and Gleb Yushin (2011). "A major constituent of brown algae for use in high-capacity Li-ion batteries". In: *Science*, p. 1209150.

Larché, F and John W Cahn (1973). "A linear theory of thermochemical equilibrium of solids under stress". In: *Acta metallurgica* 21.8, pp. 1051–1063.

Li, James Chen-Min (1978). "Physical chemistry of some microstructural phenomena". In: *Metallurgical Transactions A* 9.10, pp. 1353–1380.

Limthongkul, Pimpa, Young-Il Jang, Nancy J Dudney, and Yet-Ming Chiang (2003). "Electrochemically-driven solid-state amorphization in lithium-silicon alloys and implications for lithium storage". In: *Acta Materialia* 51.4, pp. 1103–1113.

Liu, G, H Zheng, S Kim, Y Deng, AM Minor, X Song, and VS Battaglia (2008). "Effects of various conductive additive and polymeric binder contents on the performance of a lithium-ion composite cathode". In: *Journal of The Electrochemical Society* 155.12, A887–A892.

Liu, Wei-Ren, Mo-Hua Yang, Hung-Chun Wu, SM Chiao, and Nae-Lih Wu (2005). "Enhanced cycle life of Si anode for Li-ion batteries by using modified elastomeric binder". In: *Electrochemical and Solid-State Letters* 8.2, A100–A103.

McDowell, Matthew T, Seok Woo Lee, William D Nix, and Yi Cui (2013). "25th anniversary article: understanding the lithiation of silicon and other alloying anodes for lithium-ion batteries". In: *Advanced Materials* 25.36, pp. 4966–4985.

Park, Mi-Hee, Min Gyu Kim, Jaebum Joo, Kitae Kim, Jeyoung Kim, Soonho Ahn, Yi Cui, and Jaephil Cho (2009). "Silicon nanotube battery anodes". In: *Nano letters* 9.11, pp. 3844–3847.

Prussin, S (1961). "Generation and distribution of dislocations by solute diffusion". In: *Journal of Applied Physics* 32.10, pp. 1876–1881.

Rhodes, Kevin, Nancy Dudney, Edgar Lara-Curzio, and Claus Daniel (2010). "Understanding the degradation of silicon electrodes for lithium-ion batteries using acoustic emission". In: *Journal of the Electrochemical Society* 157.12, A1354–A1360.

Santimetaneedol, Arnuparp, Rajasekhar Tripuraneni, Shawn A Chester, and Siva PV Nadimpalli (2016). "Time-dependent deformation behavior of polyvinylidene fluoride binder: Implications on the mechanics of composite electrodes". In: *Journal of Power Sources* 332, pp. 118–128.

Singh, Gaurav and Tanmay K Bhandakkar (2017). "Analytical Investigation of Binder's Role on the Diffusion Induced Stresses in Lithium Ion Battery through a Representative System of Spherical Isolated Electrode Particle Enclosed by Binder". In: *Journal of The Electrochemical Society* 164.4, A608–A621.

Song, Jiangxuan, Mingjiong Zhou, Ran Yi, Terrence Xu, Mikhail L Gordin, Duihai Tang, Zhaoxin Yu, Michael Regula, and Donghai Wang (2014). "Interpenetrated gel polymer binder for high-performance silicon anodes in lithium-ion batteries". In: *Advanced Functional Materials* 24.37, pp. 5904–5910.

Song, Yicheng, Bo Lu, Xiang Ji, and Junqian Zhang (2012). "Diffusion induced stresses in cylindrical lithium-ion batteries: analytical solutions and design insights". In: *Journal of The Electrochemical Society* 159.12, A2060–A2068.

Takahashi, Kenji, Kenneth Higa, Sunil Mair, Mahati Chintapalli, Nitash Balsara, and Venkat Srinivasan (2016). "Mechanical degradation of graphite/PVDF composite electrodes: a model-experimental study". In: *Journal of The Electrochemical Society* 163.3, A385–A395.

Whittingham, M Stanley (2012). "History, evolution, and future status of energy storage". In: *Proceedings of the IEEE* 100.Special Centennial Issue, pp. 1518–1534.

Wu, Mingyan, Xingcheng Xiao, Nenad Vukmirovic, Shidi Xun, Prodip K Das, Xiangyun Song, Paul Olalde-Velasco, Dongdong Wang, Adam Z Weber, Lin-Wang Wang, et al. (2013). "Toward an ideal polymer binder design for high-capacity battery anodes". In: *Journal of the American Chemical Society* 135.32, pp. 12048–12056.

Wu, Wei, Xinran Xiao, Miao Wang, and Xiaosong Huang (2014). "A microstructural resolved model for the stress analysis of lithium-ion batteries". In: *Journal of The Electrochemical Society* 161.5, A803–A813.

Yang, Fuqian (2005). "Interaction between diffusion and chemical stresses". In: *Materials Science and Engineering: A* 409.1-2, pp. 153–159.

Zang, Jin-Liang and Ya-Pu Zhao (2012a). "A diffusion and curvature dependent surface elastic model with application to stress analysis of anode in lithium ion battery". In: *International Journal of Engineering Science* 61, pp. 156–170.

— (2012b). "Silicon nanowire reinforced by single-walled carbon nanotube and its applications to anti-pulverization electrode in lithium ion battery". In: *Composites Part B: Engineering* 43.1, pp. 76–82.

Zhang, Kai, Yong Li, Bailin Zheng, Gangpeng Wu, Jingshen Wu, and Fuqian Yang (2017). "Large deformation analysis of diffusion-induced buckling of nanowires in lithium-ion batteries". In: *International Journal of Solids and Structures* 108, pp. 230–243.

Zhang, Xiangchun, Wei Shyy, and Ann Marie Sastry (2007). "Numerical simulation of intercalation-induced stress in Li-ion battery electrode particles". In: *Journal of the Electrochemical Society* 154.10, A910–A916.

Zhao, Kejie, Matt Pharr, Shengqiang Cai, Joost J Vlassak, and Zhigang Suo (2011). "Large plastic deformation in high-capacity lithium-ion batteries caused by charge and discharge". In: *Journal of the American Ceramic Society* 94, s226–s235.